HHS Public Access

Author manuscript

Anal Chem. Author manuscript; available in PMC 2019 January 16.

Published in final edited form as:

Anal Chem. 2018 January 16; 90(2): 1217–1222. doi:10.1021/acs.analchem.7b03901.

Metabolic Measurements of Non-permeating Compounds in Live Cells Using Hyperpolarized NMR

Mengxiao Liu and **Christian Hilty***

Department of Chemistry, Texas A&M University, 3255 TAMU, College Station, TX 77843, USA

Abstract

Hyperpolarization by dissolution dynamic nuclear polarization (D-DNP) has emerged as a technique for enhancing NMR signals by several orders of magnitude, thereby facilitating the characterization of metabolic pathways both *in vivo* and *in vitro*. Following the introduction of an externally hyperpolarized compound, real-time NMR enables the measurement of metabolic flux in the corresponding pathway. Spin relaxation however limits the maximum experimental time and prevents the use of this method with compounds exhibiting slow membrane transport rates. Here, we demonstrate that electroporation can serve as a method for membrane permeabilization for use with D-DNP in cell cultures. An electroporation apparatus hyphenated with stopped flow sample injection permits the introduction of the hyperpolarized metabolite within 3 s after the electrical pulse. In yeast cells that do not readily take up pyruvate, the addition of the electroporation pulse to the D-DNP experiment increases the signals of the downstream metabolic products CO_2 and HCO_3^-, which otherwise are near the detection limit, by 8.2 and 8.6-fold. Modeling of the time dependence of these signals then permits the determination of the respective kinetic rate constants. The observed conversion rate from pyruvate to CO_2 normalized for cell density was found to increase by a factor of 12 due to the alleviation of the membrane transport limitation. Using electroporation therefore extends the applicability of D-DNP to *in vitro* studies to a wider range of metabolites, and at the same time reduces the influence of membrane transport on the observed conversion rates.

Graphical Abstract

*Corresponding Author: chilty@tamu.edu.

Supporting Information

The Supporting Information is available free of charge on the ACS Publications website. Figures of additional pyruvate and glucose experiments, and fluorescence images of dye stained electroporated yeast cells are provided.

The authors declare no competing financial interest.

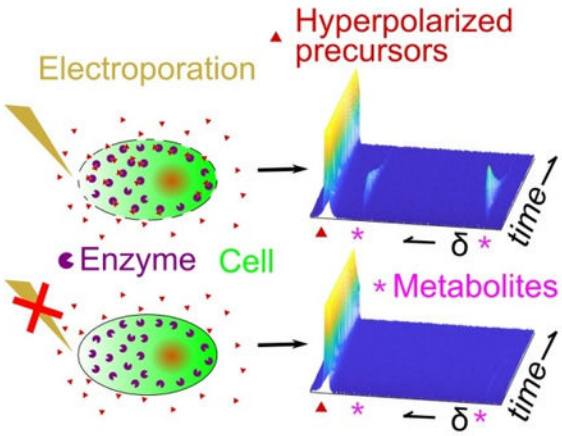

Nuclear magnetic resonance (NMR), a spectroscopic technique capable of recognizing chemical identities even in complex mixtures, has long been applied to the determination of metabolic products and kinetics.[1–3] More recently, hyperpolarization of nuclear spins has been introduced as a method of enhancing signals and extending the reach of NMR to the characterization of metabolic pathways at an overall metabolite concentration that is reduced by several orders of magnitude compared to conventional non-hyperpolarized experiments.[4–6] Dissolution dynamic nuclear polarization (D-DNP) is a hyperpolarization technique that utilizes the larger electron Zeeman splitting, "transferring" the higher electron spin polarization to nuclear spins. This polarization process occurs at a low temperature in a magnetic field, after which hyperpolarized aliquots are dissolved and can be transferred to the NMR detector at room temperature.[7–9] In combination with magnetic resonance imaging (MRI), metabolic turnover of substrates such as pyruvate can readily be monitored *in vivo*.[10,11] D-DNP has also emerged as a tool capable of characterizing metabolic flux *in vitro*, either in perfused organs or in cell cultures.[12,13] These *in vitro* experiments have been used for basic metabolic characterization of cell lines, as well as for the development of methods for later use in *in vivo* MRI.[13]

The D-DNP experiment differs from conventional non-hyperpolarized NMR in that the observed signals stem from the polarization generated prior to the start of data acquisition. The initially high signals, therefore, need to be acquired within the time frame of nuclear spin relaxation, which typically is on the order of seconds to tens of seconds.[4] Signal averaging is not possible, but data can be measured at multiple time points when using small-flip angle excitation. These conditions result in a short overall time scale of the experiment. For determining kinetics in systems containing multiple pathways, the ability to use a short time window may be beneficial in reducing the complexity of the problem. At the same time, the observation is limited to rapid processes.[14]

Since hyperpolarization by D-DNP occurs externally, the first potentially rate-limiting step in an experiment aiming at the elucidation of metabolism is the uptake of the metabolite into cells. Membrane transport is highly dependent on active transporters that differ among cell types.[15] A method for introducing small molecules into cells is electroporation. Hyperpolarized $^{133}Cs^{+}$ has been used to probe cellular membrane impairment of pre-loaded

electroporated yeast cells.[16] Here, we introduce a method, where electroporation is hyphenated with stopped-flow sample injection and NMR detection. Electroporation allows for the introduction of arbitrary metabolites in cell cultures, compatible with D-DNP hyperpolarization. We demonstrate the measurement of the kinetics of pyruvate metabolism in yeast, a metabolite that is not readily transported into these cells. Finally, we discuss the application of this method for the determination of metabolic flux under *in vitro* conditions.

EXPERIMENTAL SECTION

Cell Preparation.

Wild yeast strain W303 cells were grown in 50 mL culturing medium in a 125 mL Erlenmeyer flask. The culturing medium was prepared by dissolving 10 g yeast extract, 20 g peptone, and 20 g glucose in 1 L water. Cells were cultured in an incubating shaker at 300 rpm and 30 ºC, until the optical density at 600 nm (OD^{600}) ≈ 1.8 was reached. The cells were then collected by centrifugation at 447 g for 1 min, and dispersed in 45 mL culturing medium without glucose. This rinsing procedure was repeated twice to remove glucose. After each step, cells were collected by centrifugation. The final cell concentration was adjusted by adding culturing medium without glucose to reach a linearly extrapolated value for OD^{600} of ≈ 400 (the OD was measured at 500-fold dilution).

Hyperpolarization.

The hyperpolarized samples consisted of 0.89 M [1-^{13}C]-pyruvate (Cambridge Isotope Laboratories, Andover, MA), 15 mM tris[8-carboxy-2,2,6,6-tetrakis(2-hydroxyethyl)benzo[1,2-d:4,5-d']bis[1,3]-dithiol-4-yl]methyl free radical sodium salt (OX063; Oxford Instruments, Abingdon, U.K.), and 0.5 mM gadolinium diethylenetriaminepentaacetic acid in a solvent consisting of 3:2 v/v ethylene glycol / D_2O. Sample aliquots of 5 μL volume were hyperpolarized on ^{13}C by irradiation of microwaves with 60 mW power and 93.974 GHz frequency, at a temperature of 1.4 K in a HyperSense DNP polarizer (Oxford Instruments). The polarization time was 3 hours.

Sample Injection and Electroporation.

400 μL of the concentrated yeast cell culture in medium without glucose was pre-loaded into an electroporation cuvette with 2 mm gap (Phenix Research Products, Candler, North Carolina). The cuvette was located in an electrically insulated housing ex-situ to the NMR instrument (Figure 1). The cuvette was connected with electrical leads to the electroporator (Model 2510, Eppendorf, Germany). Tubing (0.8 mm inner diameter) was installed in the bottom of the cuvette to connect it to the sample injection system. For dissolution of the hyperpolarized sample, 4 mL pure water was heated until the vapor pressure reached 10^6 Pa. Under these conditions, the solvent reached a final temperature of approximately 160 ºC before entering the cryogenic region of the DNP polarizer. Immediately before dissolution occurred, an electroporation pulse of 1600 V was applied to the cell suspension. The hyperpolarized pyruvate sample was then dissolved, and the solution was automatically collected into a sample loop (Loop1 in Figure 1). The electroporated cells were drawn through the pre-installed tubing into a second sample loop (Loop2), using vacuum produced by a syringe. Subsequently, two injection valves connected to the respective loops were

switched, and the cell suspension and pyruvate solution were simultaneously driven into the flow cell inside the magnet. The driving force was provided by water from two high pressure pumps. This sample injection followed previously described procedures.[17] During injection, cells and hyperpolarized pyruvate solution mixed within a Y-connector mixer. This mixing occurred 2 to 3 s after the electroporation pulse. After a total injection time of 760 ms, the sample mixture arrived in the NMR flow cell. The injection valves were switched to their original positions to stop flow, and the pumps were stopped. Control experiments were performed using the same procedures, but without applying the electroporation pulse. In all experiments, the final concentration of pyruvate was 10 mM, and the cell density was diluted by 50 % compared to the density loaded into the cuvette. These final concentrations and dilutions were determined before the D-DNP experiment, using dimethyl sulfoxide as a reference compound.

Viability after electroporation was determined in separate experiments by counting colony-forming units. Cells with and without electroporation were collected and diluted to $OD^{600} \approx 3.5 \cdot 10^{-5}$. A volume of 100 μL was inoculated to agar plates. Colony-forming units were counted after incubation at 30 ºC for 48 hours.

NMR Spectroscopy.

The flow cell was positioned inside a triple resonance TXI probe installed in a 400 MHz NMR spectrometer (Bruker Biospin, Billerica, MA). After injection and following a stabilization time of 500 ms, a series of small flip angle pulses was applied to observe ^{13}C NMR spectra of the metabolic reactions in real time. The pulse sequence consisted of [G_z–P_α – acquire], and was repeated 32 times at an interval of 5 s between subsequent pulses. The pulse P_α was adjusted for a flip angle $\alpha = 30^o$ and had a pulse strength of $(\gamma B_1)/2\pi$ = 17.86 kHz, where B_1 is the amplitude of the excitation radio frequency field. For each scan, 11028 complex points were collected. A pulsed field gradient G_z (45.5 G/cm, 1 ms) was applied to remove remaining coherence before each new scan.

Data Analysis.

Raw FID data were Fourier transformed after applying an exponential window function with 2 Hz line broadening and phase corrected using the TOPSPIN program (Bruker Biospin). Peak integration and fitting of signal intensities were performed with MATLAB (The MathWorks, Natick, MA). Before integration, a linear baseline correction was applied for each peak, defined by baseline points on either side of the peak.

RESULTS AND DISCUSSION

After the mixture of hyperpolarized [1-^{13}C]-pyruvate and electroporated yeast cells arrives in the NMR probe, the buildup of the metabolic products is readily observable (Figure 2a). The individual signals are best identified by considering an individual spectrum of this time series. The spectrum measured 15.5 s after injection is displayed in Figure 2b. The pyruvate C1 signal can be seen at 170.4 ppm, as well as the predominant products CO_2 (124.8 ppm) and HCO_3^- (160.4 ppm) at intensities that are 96 and 225 times lower than the pyruvate signal. These relative signal intensities depend on the overall metabolic activity of the cells,

and also on the cell density. Signals from C2 and C3 of pyruvate, which are unlabeled, are also visible. Integrals of these signals are approximately 100-fold lower, and additionally the signals are split due to the ^{1}H-^{13}C coupling. Nevertheless, the initially high enhancement in signal to noise ratio and concomitantly the dynamic range of the hyperpolarized experiment suffice for observing these signals.

In contrast, signal intensities of CO_2 and HCO_3^- are lower by factors of 8.2 and 8.6, respectively, without electroporation (Figures 2c and d). This difference is despite hyperpolarization levels of pyruvate differing by less than 4 % in the two experiments with and without electroporation that are shown. The repeatability of the experiment is further validated by two additional sets of data, each comprising an experiment with and without electroporation (see Figure S1 in Supporting Information). The difference between the data in Figure 2a and c therefore can be attributed to the electroporation pulse. Such a difference is anticipated, since the cells were cultured with glucose before the NMR experiment. Under these growth conditions, the lactate / pyruvate permease that would be capable of transporting these compounds is not expressed or is degraded, leaving pyruvate to pass the plasma membrane only through simple diffusion.[18] These yeast cells do not readily take up pyruvate through the cell membrane, but nevertheless contain pyruvate decarboxylase in the cytosol.[19] Therefore, in the experiments described here, CO_2 can only be produced in substantial quantity if the diffusion barrier of the membrane is removed by the electroporation pulse. Under the catalytic action of the enzyme carbonic anhydrase, HCO_3^- is further produced from CO_2. On the other hand, pyruvate hydrate, which is formed non-metabolically in aqueous solution, appears in both experiments.

The near absence of membrane transport for pyruvate into the yeast cells used here stands in contrast to other metabolites, such as glucose and fructose. Unlike pyruvate, these metabolites can be taken up into yeast cells actively.[20] Meier *et al.* readily observed metabolic products after mixing with hyperpolarized glucose and fructose, and were able to visualize the respective pathways.[21] Experiments with hyperpolarized glucose performed using the protocols described here are shown in Figure S2. In these experiments, the amount of yeast cells is about 10 times smaller than in ref. 21, and otherwise experiments are comparable. The difference in the maximum product signal intensity when using hyperpolarized glucose with or without electroporation is only approximately 30 %. This result is expected, when the membrane transport is not the rate limiting step.

In general, it is necessary to consider the internal compartmentalization of the cells in any experiment, where metabolites are introduced externally. Pyruvate is converted to CO_2 by the enzyme pyruvate decarboxylase, which is primarily located in the cytosol.[19,22] It can also enter the tricarboxylic acid cycle to form CO_2 by the action of pyruvate dehydrogenase in the mitochondria. When the pyruvate concentration is high, the cytosolic pathway was reported as dominant.[22] Therefore, in the present experiments, the kinetics of introduction into mitochondria was not further considered.

In order to quantify the differences observed with and without electroporation, the reaction model in Scheme 1 was used to fit the observed signals. In this model, the rate constant for transport of pyruvate to the intracellular environment is included in the apparent first order

rate constant $k(\text{pyr}\rightarrow\text{CO}_2)$.[5,23] This first order assumption holds, when the substrate concentration [substrate] << K_M of the enzyme. When only a small fraction of substrate is consumed, this rate constant can also approximate a zeroth order reaction, where the enzyme operates at $V_{\max} = k \cdot [\text{substrate}]_0$.

Between two successive pulses, NMR signals evolve following kinetic rate expressions and spin relaxation. For pyruvate, the signal depletion is dependent on relaxation and consumption due to the reaction, $\mathrm{d}S(\text{pyr})/\mathrm{dt} = -[R_1(\text{pyr}) + k(\text{pyr}\rightarrow\text{CO}_2)]S(\text{pyr})$. The signal of CO_2 increases because of production from pyruvate and decreases due to conversion to HCO_3^- and relaxation, $\mathrm{d}S(\text{CO}_2)/\mathrm{dt} = k(\text{pyr}\rightarrow\text{CO}_2)S(\text{pyr}) - [R_1(\text{CO}_2) + k(\text{CO}_2\rightarrow\text{HCO}_3^-)]S(\text{CO}_2)$. HCO_3^- is produced from CO_2, and the signal decays via relaxation, $\mathrm{d}S(\text{HCO}_3^-)/\mathrm{dt} = k(\text{CO}_2\rightarrow\text{HCO}_3^-)S(\text{CO}_2) - R_1(\text{HCO}_3^-)S(\text{HCO}_3^-)$. The excitation pulses cause an additional signal depletion of a factor of cos(α) for each pulse with flip angle α.

For fitting of this model to the observed signals, only the labeled C1 position in pyruvate was considered, since the observed product peaks originate from this carbon atom. $R_1(\text{pyr})$ and $k(\text{CO}_2\rightarrow\text{HCO}_3^-)$ are assumed to be the same with and without electroporation, since the fraction of pyruvate consumed is small and no plasma membrane transport is expected for the conversion step $CO_2\rightarrow HCO_3^-$. Therefore, an experiment with and an experiment without electroporation were combined into one set of data and fitted with six signal curves simultaneously. The two experiments in the set share the common unknown parameters $R_1(\text{pyr})$ and $k(\text{CO}_2\rightarrow\text{HCO}_3^-)$, but are described by different $k(\text{pyr}\rightarrow\text{CO}_2)$. The fitted T_1 relaxation and kinetic rate constants were obtained by minimizing the sum of residual squares between calculated and measured data points. As in previous studies,[24–26] the signal of pyruvate hydrate is not included in the fitting. Pyruvate hydrate results from the reversible hydration of pyruvate in a non-enzymatic process and is not metabolized.[10] Its signal is less than 2 % of pyruvate in the present experiments. The results from three sets of data are shown in Figure 3, and the rate constants are given in the figure caption. Since the loaded cell concentrations differ slightly in each experiment, the rate constant values from each set of data were normalized to the final cell concentrations as determined by OD of the loaded cell suspension and the dilution factor during sample injection, and averaged. The result for $k(\text{pyr}\rightarrow\text{CO}_2)$ is $(4.71 \pm 0.86) \cdot 10^{-6}\ \text{s}^{-1}\cdot\text{OD}^{-1}$ with electroporation and $(4.11 \pm 1.67) \cdot 10^{-7}\ \text{s}^{-1}\cdot\text{OD}^{-1}$ without electroporation. The fitted value for $k(\text{CO}_2\rightarrow\text{HCO}_3^-)$ is $(3.20 \pm 0.19) \cdot 10^{-4}\ \text{s}^{-1}\cdot\text{OD}^{-1}$. The errors indicated are the standard deviations from three sets of data. The cell density of W303 strain is about $2 \cdot 10^7$ cell / mL when $\text{OD}^{600} = 1$.[27] Therefore, the approximate observed values for the rate constants expressed per cell are $k(\text{pyr}\rightarrow\text{CO}_2) = 2.35 \cdot 10^{-13}\ \text{s}^{-1}\cdot\text{cell}^{-1}$ with electroporation and $2.05 \cdot 10^{-14}\ \text{s}^{-1}\cdot\text{cell}^{-1}$ without electroporation, and $k(\text{CO}_2\rightarrow\text{HCO}_3^-) = 1.60 \cdot 10^{-11}\ \text{s}^{-1}\cdot\text{cell}^{-1}$.

These numbers indicate that $k(\text{pyr}\rightarrow\text{CO}_2)$ increases about twelve times through the use of electroporation to render the plasma membrane permeable. Based on these results, electroporation is shown to be an effective method to introduce hyperpolarized metabolites into cells in the absence of natural membrane transporters. The hyphenated electroporation system does not impose an additional delay time to the automatic liquid driven injection system, by collecting the ex-situ electroporated cells into the second sample loop. This

method is therefore compatible with any compounds that can be hyperpolarized by D-DNP. Compared to manual mixing, the automated injection results in a shorter delay, and a higher polarization level can be preserved.

The repeatability of the D-DNP experiment does not appear to be impacted by the electroporation pulse, as judged from the standard deviations. Compared to other protocols for introducing small molecules into cells, such as heat shock, the use of carriers, and overexpression of transport proteins, electroporation has several advantages.[31–34] Electroporation can introduce various molecules into any cell type with high transfer efficiency. Most importantly, preparation requirements are minimal, since other reagents or sample components (*e.g.* viral vectors or lipid vesicles) or chemical / biological processing of cells is not needed.

To ensure that cells are in best possible condition at the time of the NMR measurement after electroporation, the hyperpolarized pyruvate was mixed with the electroporated yeast cells as little as 2 – 3 s after the high voltage pulse was applied. This time duration was chosen in accordance with a variability in the charging time of < 1 s of the power supply that was employed. It would be possible to further reduce this time delay with the use of a purpose designed power supply that allows for pre-charging. It would also be possible to perform electroporation after mixing with a flow cell electroporation device.[35] However, the recovery of openings on cell membranes requires at least several seconds.[36] This recovery time was confirmed under the conditions employed here by fluorescence microscopy measurements (see Figure S3). It was found that electroporated yeast cells can be stained with the fluorescent dye even after 12 s. As a control, the dye does not enter cells without electroporation even after mixing for several minutes. Therefore, the currently achieved time delay between the electroporation pulse and mixing appears sufficient for these experiments.

A concern in the use of electroporation generally is whether cells remain viable after completion of the procedure. For yeast cells and using an electric field of 800 V/cm, viability was measured as 47 % by counting colony-forming units, which is close to a literature value of 50 %.[37] The D-DNP experiment is unique in that it probes a short time window of a few tens of seconds after electroporation. Even if cells ultimately do not remain viable, enzymes are still expected to be active. The physiological state of cells may ultimately change after electroporation, as the electric field can cause redox state changes and membrane pores can result in loss of some essential ions and small molecules.[38,39] For in cell measurements of enzyme activity, as demonstrated here on the example of enzymes in the pyruvate metabolism pathways, the electroporation based method however can be expected to yield accurate results on substrate turnover.

CONCLUSIONS

In summary, we compared signals of metabolic products after introduction of pyruvate hyperpolarized by D-DNP into yeast cells by simple mixing, or by electroporation. Electroporation alleviates the barrier for transport of metabolic precursors imposed by the cell membrane. Unlike glucose or fructose, pyruvate cannot be quickly absorbed into the yeast cells used in these experiments. As a result, simple mixing of cell suspensions with

hyperpolarized pyruvate solution only resulted in product signals close to the lower limit of detection. With electroporation, approximately 8-fold stronger signals of the products were observed. The apparent conversion rate from pyruvate to CO_2 increased by a factor of about 12. These results demonstrate that incorporating electroporation into *in vitro* D-DNP experiments reduces the influence of membrane transport on observed rate constants. At the same time, it provides a versatile method to facilitate the characterization of metabolic pathways using hyperpolarized molecules that may play vital roles in cells, but do not readily cross the cell membrane.

Supplementary Material

Refer to Web version on PubMed Central for supplementary material.

ACKNOWLEDGMENT

Financial support from the National Institutes of Health (Grant *R21-GM107927*) is gratefully acknowledged.

REFERENCES

(1). Gallinger A; Biet T; Pellerin L; Peters T Angew. Chem. Int. Ed 2011, 50 (49), 11672–11674.
(2). Larive CK; Barding GA; Dinges MM Anal. Chem 2015, 87 (1), 133–146. [PubMed: 25375201]
(3). Shestov AA; Mancuso A; Lee S-C; Guo L; Nelson DS; Roman JC; Henry P-G; Leeper DB; Blair IA; Glickson JD J. Biol. Chem 2016, 291 (10), 5157–5171. [PubMed: 26703469]
(4). Keshari KR; Wilson DM Chem. Soc. Rev 2014, 43 (5), 1627–1659. [PubMed: 24363044]
(5). Dzien P; Fages A; Jona G; Brindle KM; Schwaiger M; Frydman L J. Am. Chem. Soc 2016, 138 (37), 12278–12286. [PubMed: 27556338]
(6). Cavallari E; Carrera C; Aime S; Reineri F Chem. - Eur. J 2017, 23 (5), 1200–1204. [PubMed: 27870463]
(7). Ardenkjær-Larsen JH; Fridlund B; Gram A; Hansson G; Hansson L; Lerche MH; Servin R; Thaning M; Golman K Proc. Natl. Acad. Sci. U. S. A 2003, 100 (18), 10158–10163. [PubMed: 12930897]
(8). Ardenkjaer-Larsen J-H; Boebinger GS; Comment A; Duckett S; Edison AS; Engelke F; Griesinger C; Griffin RG; Hilty C; Maeda H; Parigi G; Prisner T; Ravera E; van Bentum J; Vega S; Webb A; Luchinat C; Schwalbe H; Frydman L Angew. Chem. Int. Ed 2015, 54 (32), 9162–9185.
(9). Lee Y Appl. Spectrosc. Rev 2016, 51 (3), 210–226.
(10). Golman K; Zandt RI; Thaning M Proc. Natl. Acad. Sci 2006, 103 (30), 11270–11275. [PubMed: 16837573]
(11). Brindle KM J. Am. Chem. Soc 2015, 137 (20), 6418–6427. [PubMed: 25950268]
(12). Lerche MH; Jensen PR; Karlsson M; Meier S Anal. Chem 2015, 87 (1), 119–132. [PubMed: 25084065]
(13). Lumata L; Yang C; Ragavan M; Carpenter N; DeBerardinis RJ; Merritt ME In Methods in Enzymology; Elsevier, 2015; Vol. 561, pp 73–106. [PubMed: 26358902]
(14). Günther UL In Modern NMR Methodology; Springer Berlin Heidelberg, 2011; Vol 335, pp 23–69.
(15). Noinaj N; Buchanan SK Curr. Opin. Struct. Biol 2014, 27, 8–15. [PubMed: 24681594]
(16). Karlsson M; Ardenkjær-Larsen JH; Lerche MH Chem Commun 2017, 53 (49), 6625–6628.
(17). Chen H-Y; Hilty C ChemPhysChem 2015, 16 (12), 2646–2652. [PubMed: 26139513]
(18). Casal M; Paiva S; Queirós O; Soares-Silva I FEMS Microbiol. Rev 2008, 32 (6), 974–994. [PubMed: 18759742]
(19). Ruiz-Amil M; Fernández MJ; Medrano L; Losada M Arch. Für Mikrobiol 1966, 55 (1), 46–53.

(20). Ozcan S; Johnston M Microbiol. Mol. Biol. Rev. MMBR 1999, 63 (3), 554–569. [PubMed: 10477308]

(21). Meier S; Karlsson M; Jensen PR; Lerche MH; Duus JØ Mol. Biosyst 2011, 7 (10), 2834. [PubMed: 21720636]

(22). Pronk JT; Yde Steensma H; Van Dijken JP Yeast 1996, 12 (16), 1607–1633. [PubMed: 9123965]

(23). Menichetti L; Frijia F; Flori A; Wiesinger F; Lionetti V; Giovannetti G; Aquaro GD; Recchia FA; Ardenkjaer-Larsen JH; Santarelli MF; Lombardi M Contrast Media Mol. Imaging 2012, 7 (1), 85–94. [PubMed: 22344884]

(24). Yang C; Harrison C; Jin ES; Chuang DT; Sherry AD; Malloy CR; Merritt ME; DeBerardinis RJ J. Biol. Chem 2014, 289 (9), 6212–6224. [PubMed: 24415759]

(25). Harrison C; Yang C; Jindal A; DeBerardinis RJ; Hooshyar MA; Merritt M; Dean Sherry A; Malloy CR NMR Biomed 2012, 25 (11), 1286–1294. [PubMed: 22451442]

(26). Harris T; Eliyahu G; Frydman L; Degani H Proc. Natl. Acad. Sci. U. S. A 2009, 106 (43), 18131–18136. [PubMed: 19826085]

(27). Kokina A; Kibilds J; Liepins J FEMS Yeast Res 2014, 14 (5), 697–707. [PubMed: 24661329]

(28). Moret S; Dyson PJ; Laurenczy G Dalton Trans 2013, 42 (13), 4353. [PubMed: 23412518]

(29). Seravalli J; Ragsdale SW Biochemistry 2008, 47 (26), 6770–6781. [PubMed: 18589895]

(30). Chattergoon N; Martínez-Santiesteban F; Handler WB; Ardenkjaer-Larsen JH; Scholl TJ Contrast Media Mol. Imaging 2013, 8 (1), 57–62. [PubMed: 23109393]

(31). Gietz RD; Schiestl RH Nat. Protoc 2007, 2 (1), 31–34. [PubMed: 17401334]

(32). Aune TEV; Aachmann FL Appl. Microbiol. Biotechnol 2010, 85 (5), 1301–1313. [PubMed: 19946685]

(33). Wang Y; Kahane S; Cutcliffe LT; Skilton RJ; Lambden PR; Clarke IN PLoS Pathog 2011, 7 (9), e1002258. [PubMed: 21966270]

(34). Li Z; Xu J; Jiang T; Ge Y; Liu P; Zhang M; Su Z; Gao C; Ma C; Xu P Sci. Rep 2016, 6 (1).

(35). Wu M; Zhao D; Zhong W; Yan H; Wang X; Liang Z; Li Z Sci. Rep 2013, 3 (1).

(36). Wang W; Foley K; Shan X; Wang S; Eaton S; Nagaraj VJ; Wiktor P; Patel U; Tao N Nat. Chem 2011, 3 (3), 251–257.

(37). Delorme E Appl. Environ. Microbiol 1989, 55 (9), 2242–2246. [PubMed: 2679384]

(38). Ho SY; Mittal GS Crit. Rev. Biotechnol 1996, 16 (4), 349–362. [PubMed: 8989868]

(39). Thrivikraman G; Boda SK; Basu B Biomaterials 2018, 150, 60–86. [PubMed: 29032331]

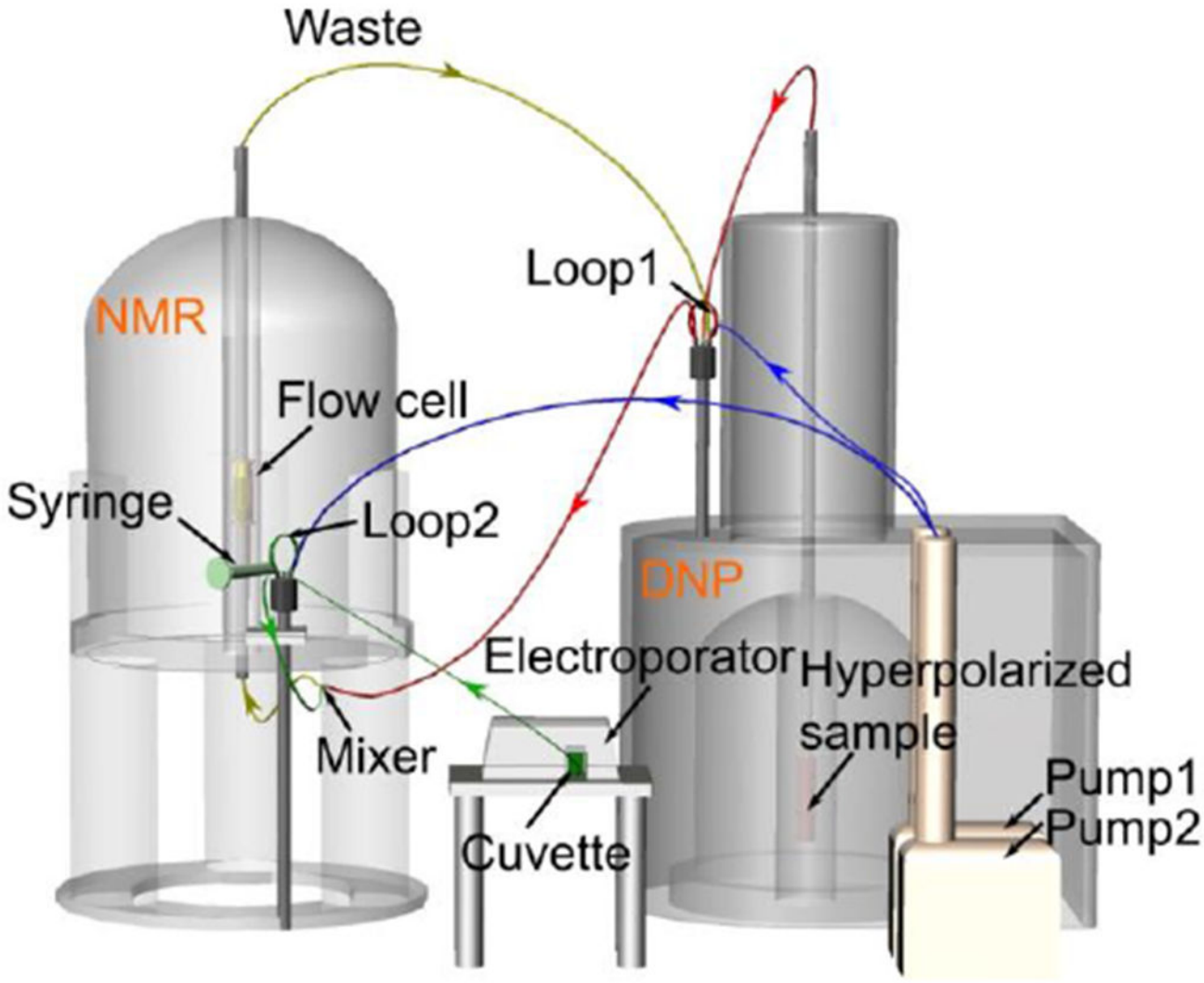

Figure 1.

Diagram of ex-situ electroporator interfaced with DNP-NMR. Red and green lines indicate the injection pathways of the hyperpolarized pyruvate and cell solutions, respectively. The flow path of the mixture is indicated with yellow lines. Blue lines indicate water used to drive the samples from the two pumps.

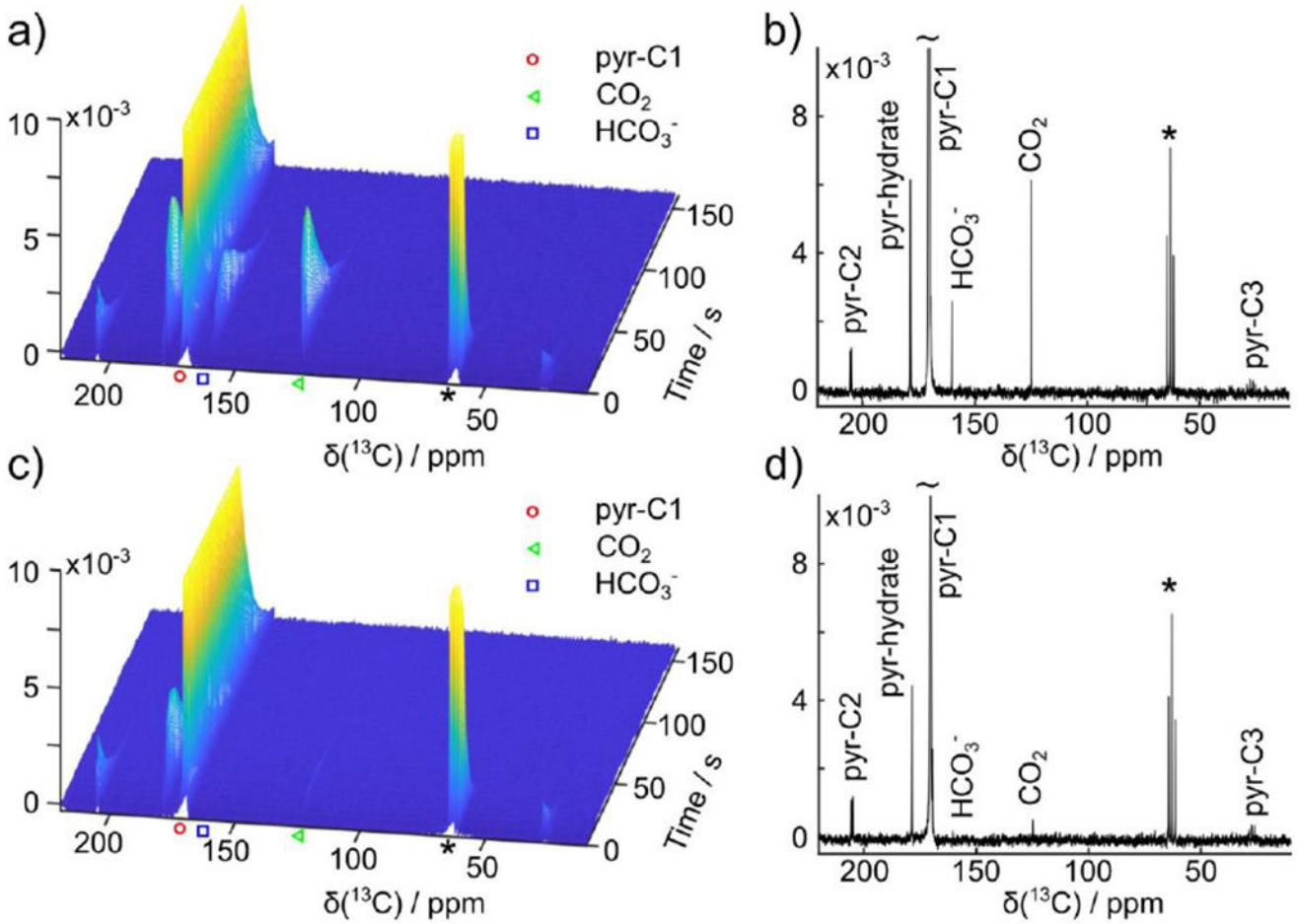

Figure 2.

a) Time series of ^{13}C NMR spectra obtained after introducing hyperpolarized [1-^{13}C]-pyruvate into electroporated yeast cells. b) 1D spectrum from the series in (a), taken at 15.5 s after injection into the flow cell. c) Time series as in (a), with omission of the electroporation pulse. d) Spectrum from (c), taken 15.5 s after injection. In all spectra, resonance peaks from C1, C2, and C3 of pyruvate are labeled as pyr-C1, pyr-C2, and pyr-C3. Pyruvate hydrate is referred to as pyr-hydrate. * indicates the solvent peak from the hyperpolarized ethylene glycol. The intensity values are shown relative to the intensity of hyperpolarized pyruvate in the first scan. Signals of pyr-C1 and * that are larger than the axis scale are cut at the top of the scale in all panels.

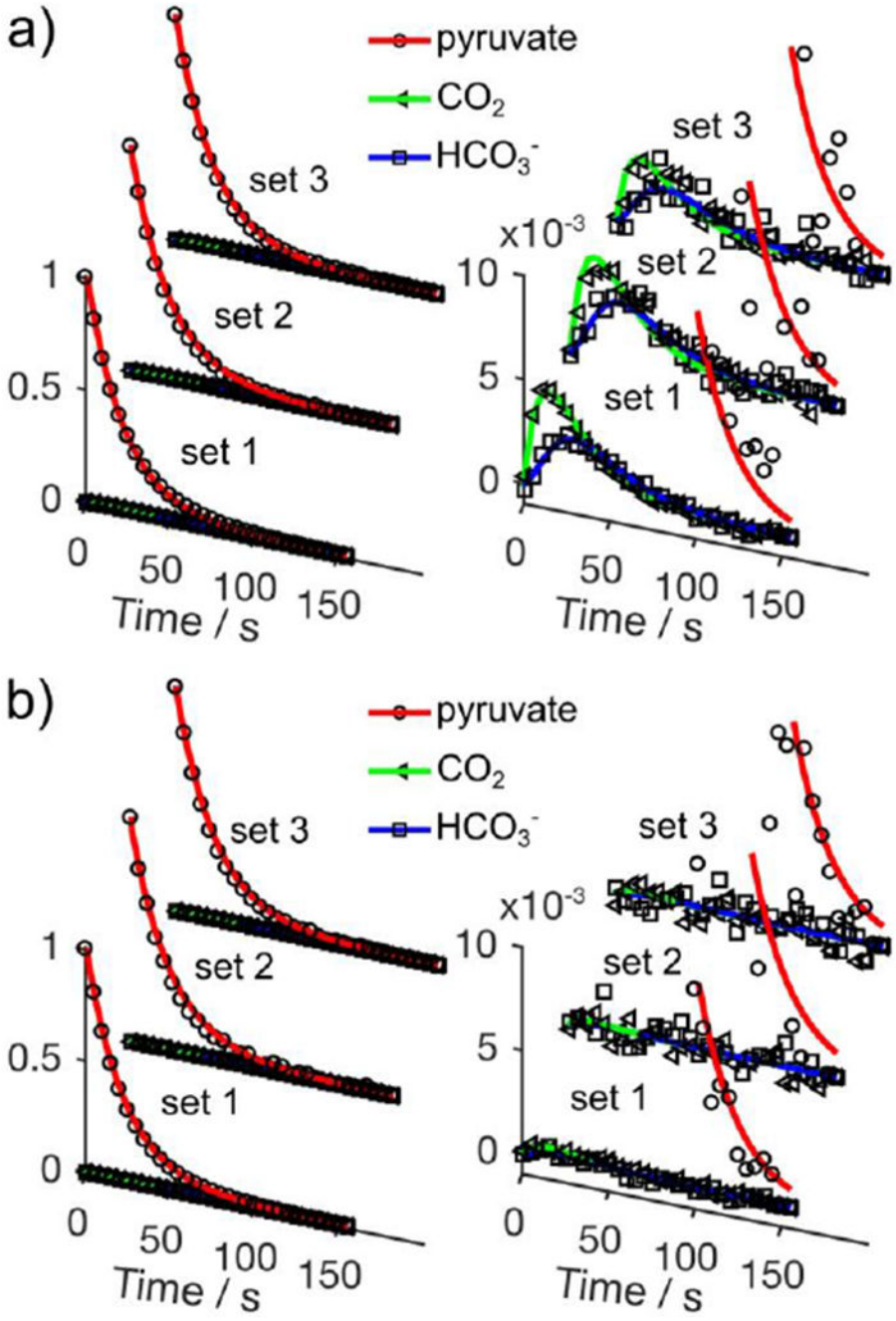

Figure 3.

Fit of NMR signal intensities in the pyruvate metabolism, using kinetic equations derived from Scheme 1. a) Electroporated yeast cells mixed with hyperpolarized [1-^{13}C]-pyruvate. b) Non-electroporated yeast cells mixed with hyperpolarized [1-^{13}C]-pyruvate. The vertical axis is enlarged in the second panel in (a) and (b) to show the time evolution of product signals. From three sets of data, each comprising an experiment with and without electroporation, optimized parameters are $k(\text{pyr}\rightarrow\text{CO}_2) = (4.96 \pm 0.14) \cdot 10^{-6}$, $(5.42 \pm 0.47) \cdot 10^{-6}$, and $(3.75 \pm 0.43) \cdot 10^{-6}$ $\text{s}^{-1}\cdot\text{OD}^{-1}$ with electroporation. $k(\text{pyr}\rightarrow\text{CO}_2) = (6.03 \pm 1.02)$

$\cdot 10^{-7}$, $(3.08 \pm 3.40) \cdot 10^{-7}$, and $(3.21 \pm 3.46) \cdot 10^{-7}$ $s^{-1} \cdot OD^{-1}$ without electroporation. $k(CO_2 \rightarrow HCO_3^-) = (3.01 \pm 0.13) \cdot 10^{-4}$, $(3.20 \pm 0.42) \cdot 10^{-4}$, and $(3.39 \pm 0.65) \cdot 10^{-4}$ $s^{-1} \cdot OD^{-1}$ was obtained. Ranges indicate 95 % fit confidence intervals calculated using the Jacobian matrix from the fitting. The large intervals of $k(pyr \rightarrow CO_2)$ without electroporation are due to the absence of the product signals under this experimental condition. Literature values $T_1(CO_2) = 50$ s and $T_1(HCO_3^-) = 24$ s were used as constants in the fit.[28–30] The fitted $T_1(pyr) = 64.3 \pm 4.3$ s, which is consistent with literature values of 42 – 68 s *in vitro*.[25,30]

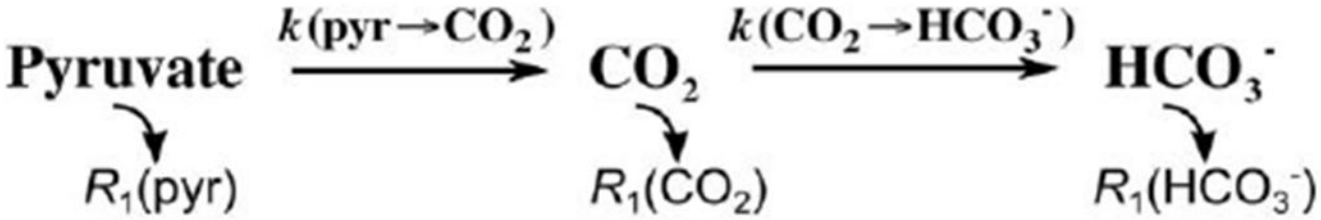

Scheme 1. Model to describe the change of NMR signal intensities [a]

[a] k(pyr→CO_2) is the conversion rate constant from pyruvate to CO_2 and k(CO_2→HCO_3^-) is the constant for conversion from CO_2 to HCO_3^-. R_1(pyr), R_1(CO_2), and R_1(HCO_3^-) are the T_1 relaxation rates for pyruvate, CO_2, and HCO_3^- respectively.